



# Evapotranspiration as a response to climate variability and ecosystem changes in southwest, China

Ali Mokhtar<sup>1,2,3</sup> · Hongming He<sup>1,2,4</sup> · Karam Alsafadi<sup>5</sup> · Yu Li<sup>6</sup> · Hongfei Zhao<sup>1,2</sup> · Soksamnang Keo<sup>1,2</sup> · Chunyu Bai<sup>1,2</sup> · Mohamed Abuarab<sup>3</sup> · Chuangjuan Zhang<sup>1,2</sup> · Khaled Elbagoury<sup>7</sup> · Jingjing Wang<sup>1,2</sup> · Qilin He<sup>1,2</sup>

Received: 7 January 2019 / Accepted: 21 May 2020 / Published online: 19 June 2020  
© Springer-Verlag GmbH Germany, part of Springer Nature 2020

## Abstract

The aim of our study is to quantify the relationship between ecosystem and climate variables in southwest China. We further examined spatiotemporal distribution patterns of daily reference evapotranspiration ( $ET_0$ ) and ecosystem types through integrated approaches, including spatiotemporal interpolation, Penman–Monteith, Mann–Kendall test, statistical correlation analysis and transition matrix based on those datasets including observation climate data, satellite remote sensing images (MODIS and Landsat) and observed ecosystem data. The following results are achieved. First, changes of  $ET_0$  were greatly influenced by the combined effects of precipitation (with a decrease rate of  $-13$  mm/10 years) and temperature (with a decrease rate of  $+0.17$  °C/10 years). The annual average  $ET_0$  increased by  $+2.1$  mm/10 years, and the increased  $ET_0$  are more than 25% of the total area. Second, evapotranspiration was regarded as a sensitive indicator of climate and ecosystem feedbacks, and these ecosystem types have a great transformation, including forest, agriculture, and grass. Forest and grass were distributed primarily in the southern and eastern mountain areas, grass was in high mountains area while agriculture was prevalent in basin areas respond to climate changes. The area of forest converted to grass was  $3670$  km<sup>2</sup>, which was greater than transition from grass to forest ( $1720$  km<sup>2</sup>). Correlation coefficients of evapotranspiration and NDVI were positive in forest and negative in agriculture. Third, the effects of these changes on climate vegetation and ecosystem process feedbacks on the quickly warming southwest China are potentially significant. Although the variation in ecosystem types was combined effects caused by climate variation and human activities, an effective ecological restoration program “Grain for Green” has improved the environmental conditions in southwest China.

**Keywords** Evapotranspiration · Climate change · Ecosystem types · Ecological restoration · NDVI

✉ Hongming He  
hongming.he@yahoo.com

✉ Yu Li  
liyuljy@163.com

<sup>1</sup> State Key Laboratory of Soil Erosion and Dry Land Farming on Loess Plateau, Institute of Soil and Water Conservation, Northwest University of Agriculture and Forestry, Yangling 712100, China

<sup>2</sup> Institute of Soil and Water Conservation, Chinese Academy of Sciences and Ministry of Water Resources, Northwest University of Agriculture and Forestry, Yangling 712100, China

<sup>3</sup> Department of Agricultural Engineering, Faculty of Agriculture, Cairo University, Giza 12613, Egypt

<sup>4</sup> School of Geographic Sciences, East China Normal University, Shanghai 210062, China

<sup>5</sup> Department of Geography and GIS, Faculty of Arts, Alexandria University, Alexandria 25435, Egypt

<sup>6</sup> Institute of Geographic Sciences and Natural Resources, Chinese Academy of Sciences, Beijing 101400, China

<sup>7</sup> Department of Agricultural Engineering, Faculty of Agriculture, Ain Shams University, Cairo 11241, Egypt

## Introduction

Global and regional climate have experienced considerable changes over the past decades which further influenced biodiversity by changing the factors of fundamental habitat such as precipitation and temperature, and resulted in hazards (Allen and Ingram 2002; Gu et al. 2007; Mantua et al. 2010; Gobron et al. 2005). Previous investigations showed although the annual average precipitation has non-significant change as a whole of China, regional and seasonal changes are obvious (Li 2011; Ye et al. 2013). In northwestern China and the middle to lower reaches of the Yangtze River, the annual precipitation presented an increasing trend, meanwhile, in southern, northeastern, and northern China, it indicated a decreasing trend (Zhai et al. 2004; Sui et al. 2013). Meanwhile, the average temperature increased by about +0.2–0.3 °C/10 year in northern China and around +0.1 °C/10 year in southern China during the past 50 years (Xu et al. 2011). The frequency of annual very warm days has increased by 1.8%, and spring and autumn turn drier since the 1990s (Ma and Ren 2007; Xu et al. 2011; Du et al. 2013).

Previous researches suggested that the variability of evapotranspiration had either negative or positive impacts on ecosystem type depending on ecosystem varieties and regional conditions (Chen et al. 2006; Bonan 2008; Thomas 2008; Fan and Thomas 2013; Jhajharia et al. 2014; Gao et al. 2015; Tony 2008; Ray et al. 2015). It indicated that vegetation cover responded to different parameters, such as climatic variables and ecosystem changes in different areas (Fabricante et al. 2009). The relationships between NDVI and climatic variables and ecosystem have been well illustrated in coupling analysis between climate and ecosystem (Li et al. 2011; Liu et al. 2013). For instance, precipitation in west China plays a vital role in ecosystems, and the correlation between vegetation conditions and precipitation are positive in most dry areas; however, heavy rainfall is negative in humid areas (Piao et al. 2004; Chen et al. 2005; Li et al. 2011; Liu et al. 2013). The impact of climate variables on NDVI is variable in the spatial distribution in southern China, and temperature changes impact much more on NDVI than on precipitation (Wang et al. 2008). In contrast, the environmental changes impact on the ecosystem variations during the past 3 decades from 1982 to 2012 in southwest China, for example, the agricultural land decreases although evergreen forest and mixed forest had an increasing trend, especially in south of Yunnan province. Agriculture area was decreased during the period from the late 1980 to 2010. It decreased by  $17.84 \times 10^4$  ha from 2000 to 2010 due to ecological restoration programs and urban construction in the agricultural area (Liu et al. 2014, Mokhtar et al. 2019).

Peng et al. (2011) studied the ecosystem changes in Guizhou province from 1970 to 2007 and indicated that the agricultural area was increased from 41 to 46% during the period of 1973–1970 and then decreased to 38% in 2002 and changed a little in 2007.

Ecosystem directly impacts the regional hydrological cycle by altering the processes of evapotranspiration and vice versa (Fang et al. 2004; Gu et al. 2007; Wang et al. 2008; Li et al. 2011). The variability of evapotranspiration across vegetation types can be attributed to mean annual climate conditions, water supply, and plant functional types. Ecosystem changes biophysical processes such as albedo, surface roughness, and the balance between sensible and latent heat loss (DeWalle et al. 2000; Jackson et al. 2001; Foley et al. 2005; Liu et al. 2008; Sun et al. 2011; Lewis 2006; Lehmann et al. 2011). Previous investigations provided a large amount of knowledge in addressing climate change patterns and its driving forces. It was examined that temporal evapotranspiration had negative trend in most of arid and semiarid stations while it was positive in humid and very humid stations using the Mann–Kendall test in 30 stations located in Iran (Khanmohammadi et al. 2017). At the national scale, changes in maximum temperature, solar radiation, and wind speed are responsible for decreasing trends of evapotranspiration in most regions of China, and decreased in many regions over the world (Gao et al. 2006; Irmak et al. 2012; Liu et al. 2012). On the other hand, at the regional scale, trends of evapotranspiration varied with location (Gong et al. 2006; Fan and Thomas 2013; Feng et al. 2014). The sunshine hours and wind speed were the main contributors to evapotranspiration changes in Sichuan Hilly Basin. Decreasing trends in evapotranspiration were found in southwestern China and Yunnan Province (Yin et al. 2010a, b; Han et al. 2012; Fan and Thomas 2013; Zhang et al. 2013; Feng et al. 2014).

The achievements of abovementioned studies improved our understandings of climate change, ecosystem changes during the past decades regionally and globally. In addressing these issues, various approaches were introduced. Specifically, evapotranspiration was estimated by various methods. Among existing methods, the Food and Agriculture Organization (FAO)56 Penman–Monteith (PM) (Allen et al. 1998), Priestley–Taylor method, the Hargreaves method, Thornthwaite methods and other empirical methods. Based on the previous studies, P–M equation was recommended as the sole standard method by FAO to calculate evapotranspiration and successfully applied in China; it incorporates both physiological and meteorological parameters and it has been widely used over the world as a result of intrinsic rationality and reliability. P–M equation is the most precise method to estimate in comparison with the alternative methods (Allen

2000; Sumner and Jacobs 2005; Suleiman et al. 2007; Kjaersgaard et al. 2008; Suyker and Verma, 2009; Wang and Zhou 2010; Fan and Thomas 2013). Therefore, in our study we have chosen Penman–Monteith (PM) for estimating evapotranspiration. The purpose of our study is to quantify relationships between ecosystem and climate variables, through integrated approaches as to explore spatiotemporal distribution patterns of daily reference evapotranspiration and ecosystem types.

## Materials and methods

### Data sources

To satisfy with investigations in this study, we collected various datasets, including climate, ecosystem types, remotely sensed images (Normalized Difference Vegetation Index, NDVI), and topography (Digital Evaluation Model, DEM). The climate data of 103 meteorological stations (1960–2016) in southwest China were from China National Meteorological Data Sharing Platform. Daily climate variables included precipitation, temperature (minimum, maximum, and average), sunshine hours, wind speed, and relative humidity. Ecosystem data (1.0 km resolution), including types and distribution, were derived from remote sensing images. These datasets were downloaded from the remotely sensed images Resource and Environment Data Cloud Platform of Chinese Academy of Sciences (<https://www.resdc.cn/>). NDVI (MOD13Q1 with resolution of 16 days and 250 m) was derived from MODIS.

### Mann–Kendall (MK) test for climate time series analysis

In this study, trend analyses of the climate variables and time series characteristics of climate variables were examined by Mann–Kendall test (M–K test,) to statistically assess if there is a monotonic upward or downward trend of the variable of interest over time (Mann 1945; Kendall 1955; Li et al. 2016). The rank-based Mann–Kendall test (M–K) is widely used to determine the significance of the trends in hydroclimatic time series (Miao et al. 2010). M–K is highly recommended for general use throughout the world due to its robustness for non-normally distributed and censored data. To detect seasonality trends, we first calculate all Kendall's tau for each season and then calculate an average Kendall's tau. The variance of the statistic can be calculated by assuming

that series are independent or dependent, which requires the calculation of a covariance.

### Penman–Monteith method for evapotranspiration ( $ET_0$ ) calculation

The Penman–Monteith equation has been recommended as the sole standard method by FAO to calculate evapotranspiration and successfully applied in China. It incorporates both physiological and meteorological parameters. As it is difficult to obtain accurate field measurements, evapotranspiration can be calculated from weather data using the P–M equation; thus, it has been widely used over the world as a result of intrinsic rationality and reliability (Allen 2000; Sumner and Jacobs 2005; Suleiman et al. 2007; Kjaersgaard et al. 2008; Suyker and Verma 2009; Wang and Zhou 2010; Fan and Thomas 2013). P–M equation considers many parameters related to the evapotranspiration process and it has presented very good results when compared to data from lysimeters populated with short grass or alfalfa. These meteorological datasets are adequate to be used in Penman–Monteith equation ( $ET_0$ ). The daily evapotranspiration values were calculated for each meteorological station. Monthly and annual evapotranspiration values were derived from the daily values. The formula of the Penman–Monteith method is described as Eq. 1

$$ET_0 = \frac{0.408 \times \Delta (R_n - G) + \gamma \times \frac{900}{T+273} \times U_2 (e_s - e_a)}{\Delta + \gamma (1 + 0.34U_2)}, \quad (1)$$

where  $ET_0$  is reference evapotranspiration (mm),  $R_n$  is the net radiation at the crop surface ( $\text{MJ m}^{-2} \text{d}^{-1}$ ),  $G$  is the soil heat flux density ( $\text{MJ m}^{-2} \text{day}^{-1}$ ),  $\Delta$  is the slope of the vapor pressure curve (kpa/C),  $\gamma$  is the psychrometric constant (kpa/C),  $T$  is the average air temperature ( $^{\circ}\text{C}$ ),  $U_2$  is wind speed measured at 2 m height (m/s),  $e_s$  is saturation vapor pressure (kPa), and  $e_a$  is actual vapor pressure (kPa). If the solar radiation  $R_s$  is not measured, it can be calculated Eq. 2 with the Angstrom formula:

$$R_{ns} = (1 - \alpha) \times R_s, \quad (2)$$

where  $R_{ns}$  is the net solar or shortwave radiation ( $\text{MJ m}^{-2} \text{day}^{-1}$ ),  $\alpha$  is the albedo or canopy reflection coefficient, which is 0.23 for the hypothetical grass reference crop [dimensionless],  $R_s$  is the incoming solar radiation ( $\text{MJ m}^{-2} \text{day}^{-1}$ ): Eq. 3

$$R_s = \left( a_s + b_s \frac{n}{N} \right) \times R_a, \quad (3)$$

where  $R_s$  is the solar or shortwave radiation [ $\text{MJ m}^{-2} \text{day}^{-1}$ ],  $n$  is the actual duration of sunshine [hour],  $N$  is the maximum possible duration of sunshine or daylight hours [hour],  $n/N$  is the relative sunshine duration [–],  $R_a$  is the extraterrestrial radiation [ $\text{MJ m}^{-2} \text{day}^{-1}$ ],  $a_s$  is the regression constant, expressing the fraction of extraterrestrial radiation reaching the earth on overcast days ( $n=0$ ), and  $a_s + b_s$  is the fraction of extraterrestrial radiation reaching the earth on clear days ( $n=N$ ); the Angstrom values  $a_s$  and  $b_s$  will vary. Where no actual solar radiation data are available and no calibration has been carried out for improved  $a_s$  and  $b_s$  parameters, the values  $a_s=0.25$  and  $b_s=0.50$  are recommended (Allen 2000; Sumner and Jacobs 2005; Fan and Thomas 2013). Psychrometric constant  $\gamma$  can be calculated from Eq. 4

$$\gamma = \frac{C_p \times P}{\epsilon \lambda} = 0.665 \times 10^{-3} P, \quad (4)$$

where  $\gamma$  is the psychrometric constant [ $\text{kPa C}^{-1}$ ],  $P$  is the atmospheric pressure [ $\text{kPa}$ ],  $\lambda$  is the latent heat of vaporization,  $2.45 \text{ [MJ kg}^{-1}]$ ,  $C_p$  is the specific heat at constant pressure [ $\text{MJ kg}^{-1} \text{ }^\circ\text{C}^{-1}$ ], and  $\epsilon$  is the ratio molecular weight of water vapor/dry air = 0.622 (Allen et al. 1998).

### Spatial analysis through interpolation algorithms

In this study, spatial analysis through interpolation algorithms was used to estimate spatial changes of climate variables which are becoming increasingly important as to explicit landscape and regional processes including those of regeneration, growth, and mortality of forest ecosystems. The inverse distance weighting method had the lowest mean error among the common interpolation methods. In this study, inverse distance weighting (IDW) algorithm was applied with highly variable data analysis to get the lowest mean error in comparison with the common interpolation methods which were developed by the U.S. National Weather Service in 1972 and is classified as a deterministic method. This is due to the lack of requirement in the calculation to meet specific statistical assumptions; thus, IDW is different from stochastic methods (e.g., kriging and TRA), and it is a moving average interpolator that is usually applied to highly variable data. IDW method gave the lowest mean error among the three common interpolation

methods (spline, ordinary kriging, and inverse distance weighting) (Yu et al. 2017). IDW method is also for multivariate interpolation. Its general idea is based on the assumption that the attribute value of an unsampled point is the weighted average of known values within the neighborhood (Lu and Wong 2008). This involves the process of assigning values to unknown points using values from a scattered set of known points. The value at the unknown point is a weighted sum of the values of  $N$  known points. In this study, the IDW method is used to interpolate spatial data. It can be used to estimate the unknown spatial rainfall data from the known data of sites that are adjacent to the unknown site (Goovaerts, 2000; Li and Heap 2008). The IDW formulas are presented as Eqs. 5 and 6. Furthermore, IDW does not require the preliminary modeling step of a variance distance relationship and it is very simple and quick (Moeletsi et al. 2016).

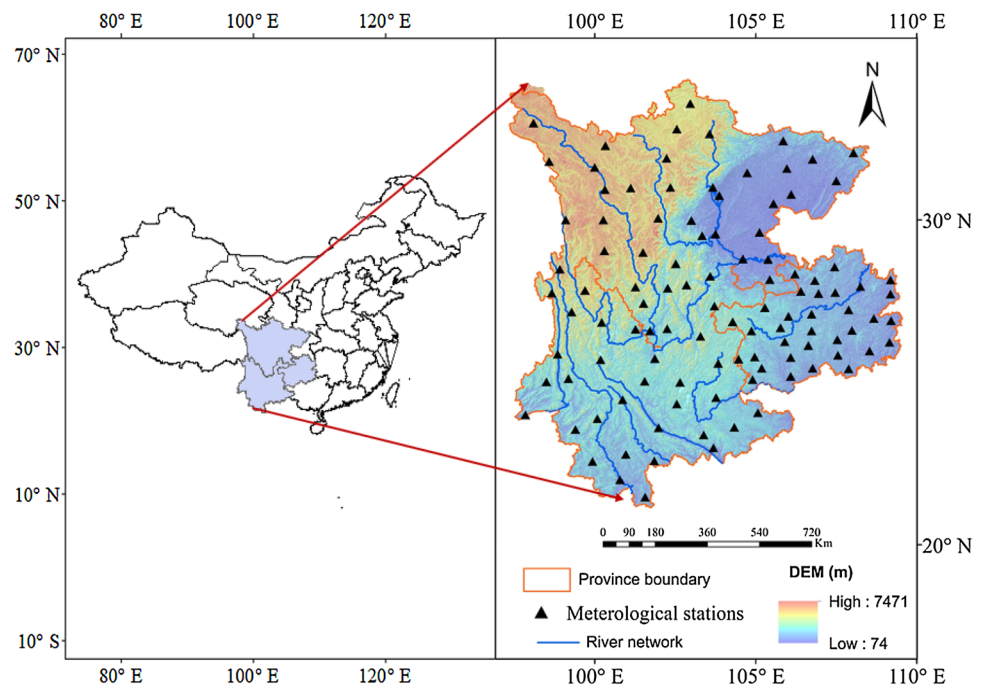
$$\hat{R}_p = \sum_{i=1}^N w_i R_i, \quad (5)$$

$$w_i = \frac{d_i^{-\alpha}}{\sum_{i=1}^N d_i^{-\alpha}}, \quad (6)$$

where  $\hat{R}_p$  is the unknown rainfall data (mm);  $R_i$  is the rainfall data of known rainfall stations (mm);  $N$  is the amount of rainfall stations;  $w_i$  is the weighting of each rainfall stations;  $d_i$  is the distance from each rainfall stations to the unknown site;  $\alpha$  is the power, and is also a control parameter, generally assumed as two as used by Zhu and Jia (2004) and Lin and Yu (2008), or as six as set by Gemmer et al. (2004).

### Study area

Our study area covers  $1,052 \times 10^6 \text{ km}^2$  of southwest China ( $21^\circ 15' \text{N}$  and  $29^\circ 25' \text{N}$ ,  $97^\circ 35' \text{E}$ – $109^\circ 59' \text{E}$ ), including Yunnan, Guizhou, and Sichuan Provinces (Fig. 1). Topographically, it can be divided into three regions, including western–Sichuan plateau, Sichuan basin, and Yunnan–Guizhou plateau. The Sichuan basin is ringed by mountains with 1000–3000 m elevation; the floor of the basin has an average elevation of 500 m. Yunnan–Guizhou plateau has an average elevation of 2000 m, it is known for its limestone karst landscape. The southwest is a typical monsoonal climate region, and divided into dry season (November–April) and

**Fig. 1** Location of the study area in southwest China

wet season (May–October), with average annual values of 15–24 °C in air temperature and 250–1400 mm in precipitation. The major ecosystem types in the southwest china are forest (46%), grass (28%), agriculture (22.8%), wetland and others (sparse forestry and grass).

## Results and discussion

### The spatiotemporal distribution of $ET_0$ (1960–2016)

Spatiotemporal distribution of  $ET_0$  in southwest China has a significant difference which resulted from complex in the topography condition and climate variables. To detect the changes of  $ET_0$ , the Penman–Monteith method was applied to investigate the spatiotemporal distribution of  $ET_0$  during the period (1960–2016). The average annual of  $ET_0$  in southwest China ranged from 840 to 1000 mm, and showed a slight increasing trend with slope +0.46 mm/year (Fig. 2a). The changing rates of  $ET_0$  (which was represented as slopes) in spring, summer, autumn, and winter were  $-0.1$ ,  $0.11$ ,  $0.35$  and  $0.11$  mm/year, respectively. Slopes are relatively higher in autumn season and lower in spring season. The changing trend of  $ET_0$  slightly decreased in spring season; however, the trends increased in the other three seasons, which agreed

with the annual trend of  $ET_0$ .  $ET_0$  is comparatively higher in the southwest of Yunnan Province, and decreases toward the Guizhou Province. Seasonally,  $ET_0$  in autumn season ranked the highest value in comparison with the different seasons, and the spring season had the lowest value.

$ET_0$  trend was carried out based on the MK test to illustrate the spatial annual trend of  $ET_0$  which ranged from  $-57$  to  $41$  mm/10 years; however, it showed an increasing trend in Yunnan province, especially in the southwest of Yunnan ( $+41$  mm/10 years) (Fig. 3a), the decreasing trend was located in the central part of Guizhou and Sichuan Basin (4.5% of total study area); the biggest decreasing trend was in Guizhou Province ( $-29$  mm/10 years). Table 1 shows the percentage area of increasing and decreasing trend over the study area. Seasonally, there was an obvious change of  $ET_0$  between dry and wet seasons although it was not a clear variation in each season, especially between autumn and winter seasons, so we selected the dry and wet seasons to present the seasonal changes on  $ET_0$ . On the one hand, in wet season it displayed a high value in Sichuan province and gradually significantly decreases toward the Guizhou province. On the other hand, dry season has no trend in most of the study area; however, there was an increasing trend in northwest of Sichuan province that agreed with previous studies (Gao et al. 2006, 2017).  $ET_0$  had a clear spatial pattern with wide

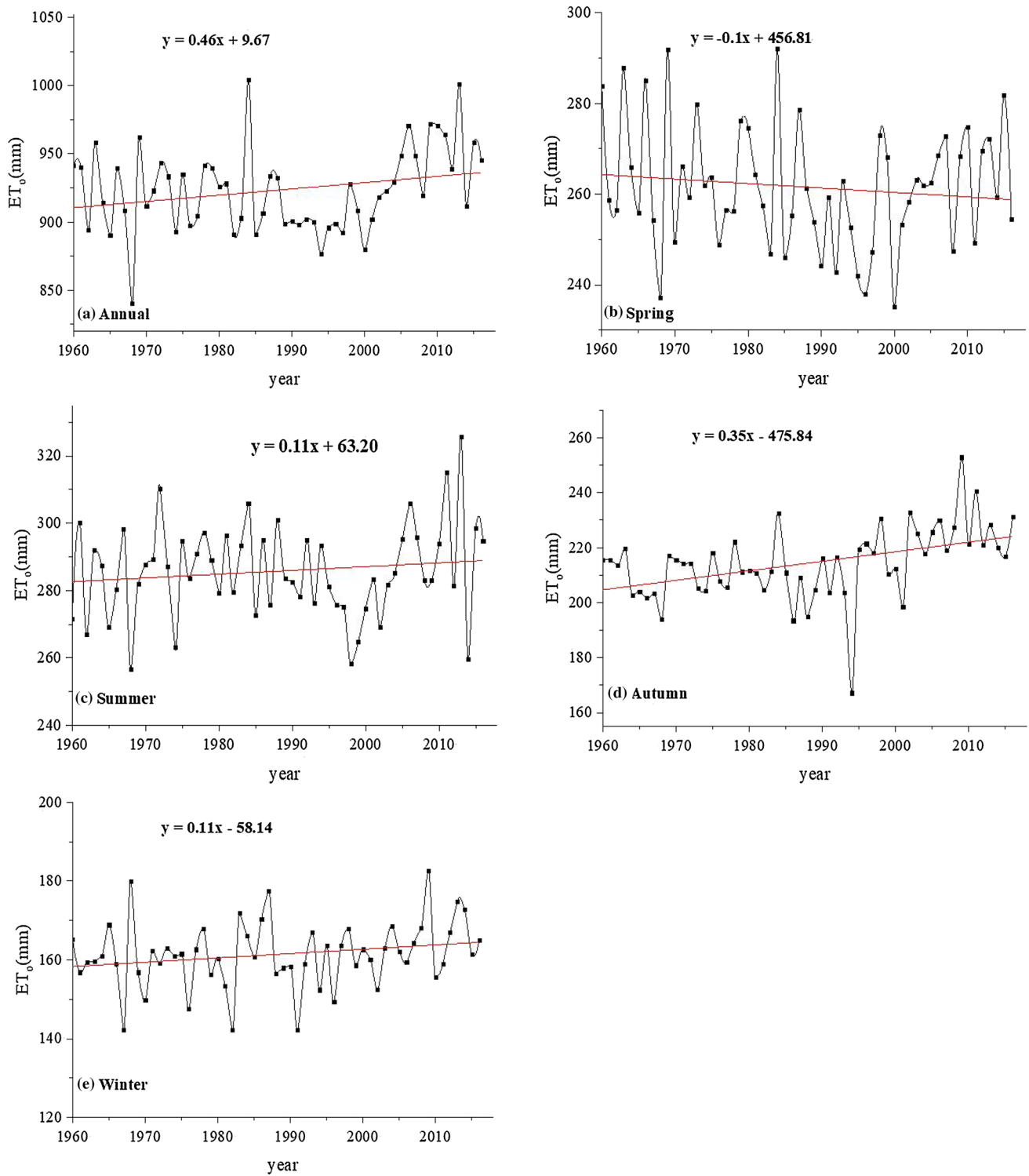


**Fig. 2** Time series analysis of  $ET_0$  in the southwest China over the past 60 years (1960–2016) (a Annual, b Spring season, c Summer season, d Autumn season, e Winter season)

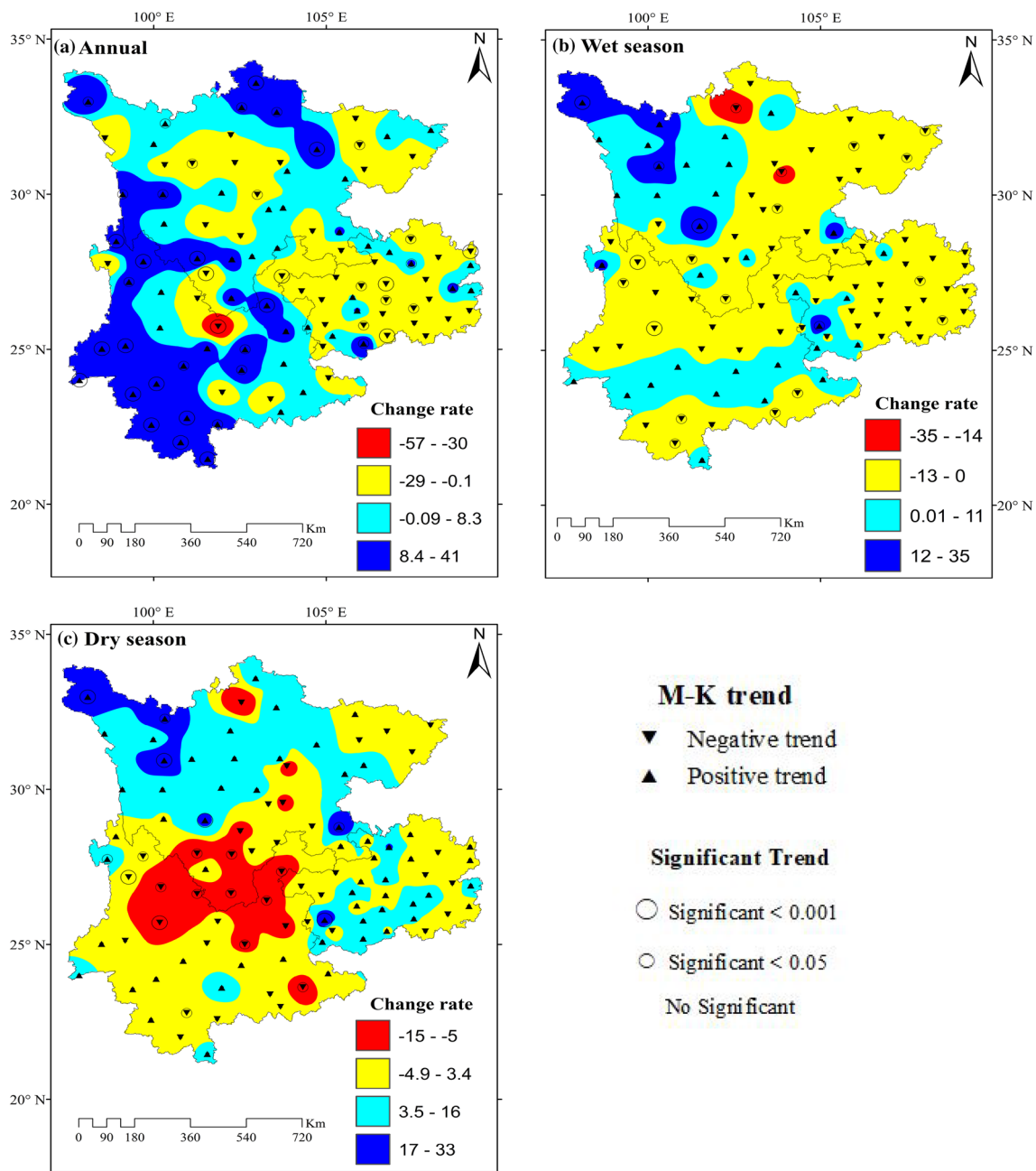


**Fig. 3** Spatial distribution analysis of annual and season  $ET_0$  over the past 60 years (1960–2016) (a Annual spatial distribution, b Wet season spatial distribution, c Dry season spatial distribution)

range because of the complex in the topography condition and different monsoon circulation branches (Thomas 1993). Significant increase of  $T_{max}$ ,  $T_{ave}$ , and  $T_{min}$ , and the decrease of relative humidity were responsible for increasing  $ET_0$ ; in contrast, the declines of wind speed and sunshine hours

played a vital role for the decreasing trend of  $ET_0$  from 1960 to 2016. The above observations are close to previous findings in southwest China (Gao et al. 2006; Zhang and Shen 2007; Yin et al. 2010a, b).

**Table 1** Statistics of changing properties for climate variables

Indices	Stations with increasing trend	Area with increasing trend (%)	Stations with decreasing trend	Area with decreasing trend (%)	Stations with no trend	Area with no trend (%)	Change in magnitude for 10 years
ATP	11	1	18	11	78	88	−13.7 mm
AAT	86	93	2	0.1	19	7	+0.17 °C
SHD	16	4	62	49	29	47	−29.4 h
RH	10	2	59	52	38	46	−0.47%
WS	23	7	53	38	31	55	−0.05 m/s
ET <sub>0</sub>	35	26.3	20	4.5	52	69.2	2.1 mm

ATP average annual precipitation, AAT average annual temperature, SHD sunshine duration, RH the relative humidity, WS the wind speed and ET<sub>0</sub> evapotranspiration

### Correlation between climate parameters and ET<sub>0</sub>

The temporal evolution of ET<sub>0</sub> rates and climate parameters has shown remarkable changes over time. The variations of climate variables contribute differently to reference evapotranspiration changes, which include temperature, vapor pressure deficit, solar radiation, and wind speed. Climate variables temporarily fluctuated and spatial distribution was rather different in southwest China during the past decades (1960–2016). Per year average slope change of climate variables was −0.20 mm precipitation (P), +0.03 °C temperature (T), −0.74 h sunshine hours (SHD), +0.03% relative humidity (RH), and −0.002 m/s wind speed (WS) (Fig. 4). The average annual precipitation is about 1040 mm with a general decrease of −7.0 mm/10 years. M–K test of statistics of changing properties for climate variables is shown in Table 1. The increasing trend of precipitation existed in 1% from the total area in the southwest China, which coincided with the previous studies of decreasing trends in this area (Liu et al. 2015). In contrast, the average annual temperature had an average increasing trend (+0.17 °C/10 years) in more than 90% of the whole area, it increased mostly in south of Yunnan Province (+0.51 °C/10 years), it sharply decreased in central of Guizhou Province by −0.14 °C/10 years based on the results from M–K test in Fig. 5. Sunshine hour duration, relative humidity, and wind speed decreased with the average rates of −29.4 h, −0.47%, and −0.05 m/s/10 years, respectively. Sunshine duration hours were the most increasing trend in southwest of Yunnan Province that reached to +66 h/10 years; however, it decreased in Guizhou Province (−110 h/10 years). Relative humidity had a decreasing trend in most of the study area, and it decreased sharply in south Yunnan Province by −1.6%/10 years. Wind speed

was complicated with general decreasing trend in the whole study area; however, it had a slight increasing trend in southwest of Yunnan (0.15 m/s per 10 years) (Fig. 5e).

However, the daily climate variables presented differently in comparison with annual distribution patterns. Maximum daily temperature ( $T_{max}$ ) increased in most regions of the study area during the period of 1960–2016, with strong influence on ET<sub>0</sub>. They had a significant increase in more than 80% of total area; in contrast, it decreased only 0.2% of total area. An increasing trend of maximum temperature was found in southwest China was +0.15 °C/10 years during the study period. The increase was clear in the high elevation regions in south Sichuan province (0.72 °C/10 years), while Guizhou with low elevation has a decreasing trend (−0.21 °C/10 years). Solar radiation has a decreasing trend (−0.06 MJ/m<sup>2</sup>/10 years). It is found that there was a significant increasing trend in small part of southwest Yunnan (0.25 MJ/m<sup>2</sup>/10 years). Strong decrease of solar radiation was found in southeast of Guizhou province which reached −0.35 MJ/m<sup>2</sup>/10 years. The vapor pressure deficit had an increasing trend (+5.3 kPa/10 years), and it was regarded as one of the major factors which impacted on ET<sub>0</sub> (Fig. 5h). It has a large increasing trend in the southwest of Yunnan (+19 kPa/10 years).

For decades, the annual temporal trend of ET<sub>0</sub> are similar to the variables that contribute the most (maximum temperature, solar radiation and vapor pressure deficit), especially with maximum temperature. The maximum temperature, solar radiation, and vapor pressure deficit have a slope +0.03 °C/year, −0.19 MJ/m<sup>2</sup>/year and −0.16 kPa/year, respectively. Maximum temperature showed a significant increasing trend while solar radiation has a strong decreasing trend, especially in 1991 and 1963, vapor pressure deficit had an increasing



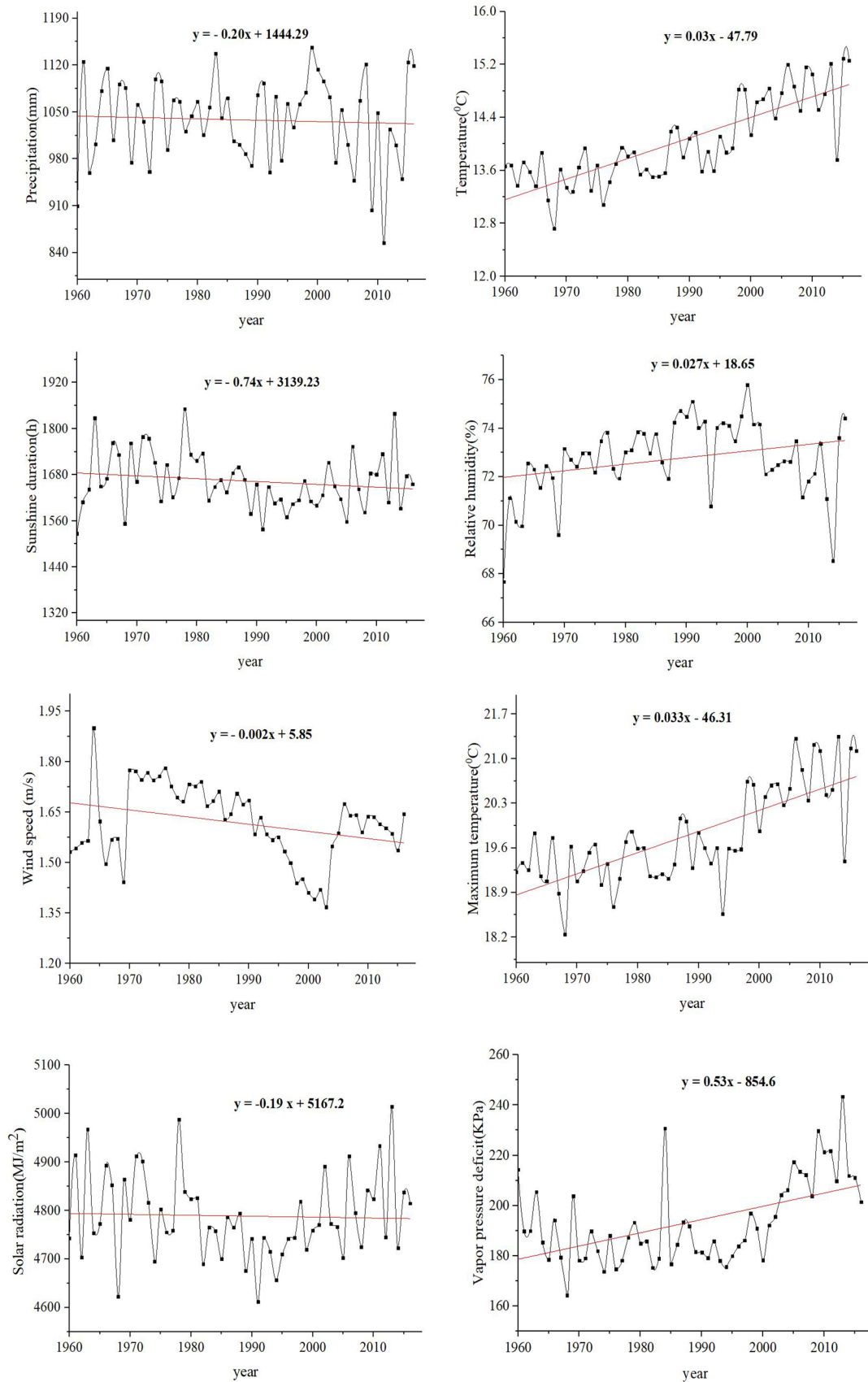


**Fig. 4** Time series analysis of climate variables over the past 60 years (1960–2016)

**Fig. 5** Spatial distribution analysis of climate variables over southwest China during (1960–2016) **(a)** Precipitation, **(b)** Temperature, **(c)** Sunshine **(d)** Relative humidity **(e)** Wind speed, **(f)** Maximum temperature, **(g)** (VPD) is the vapor pressure deficit and **(h)** Solar radiation

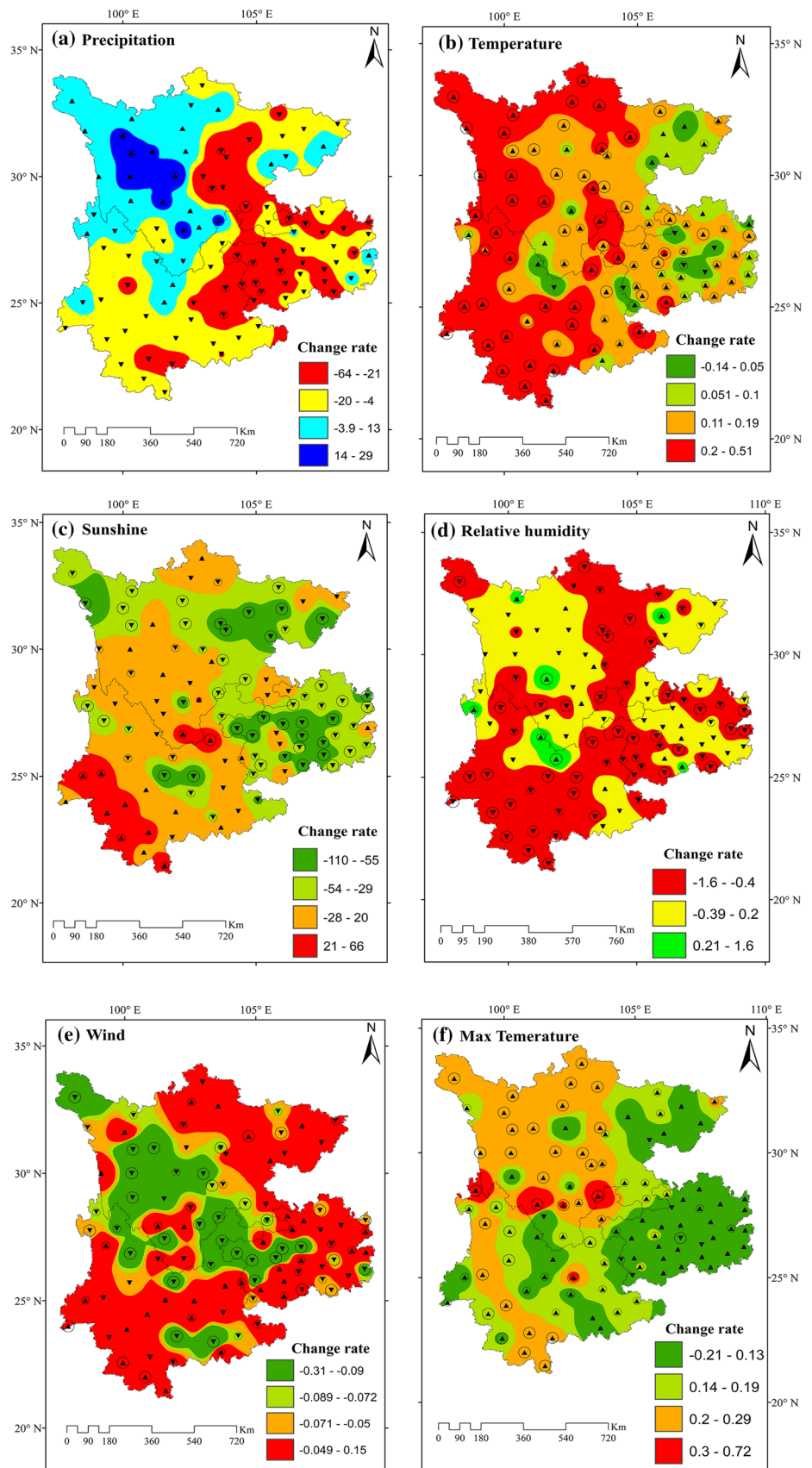
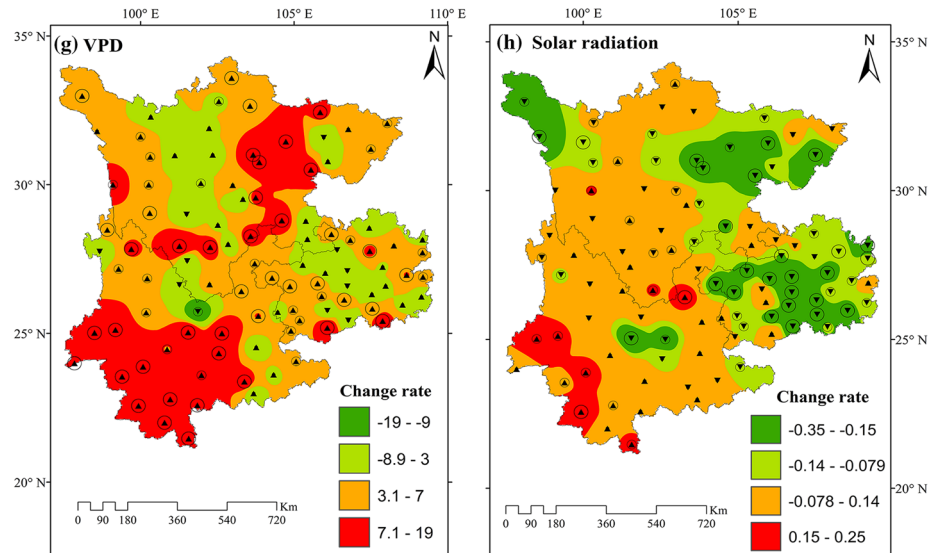


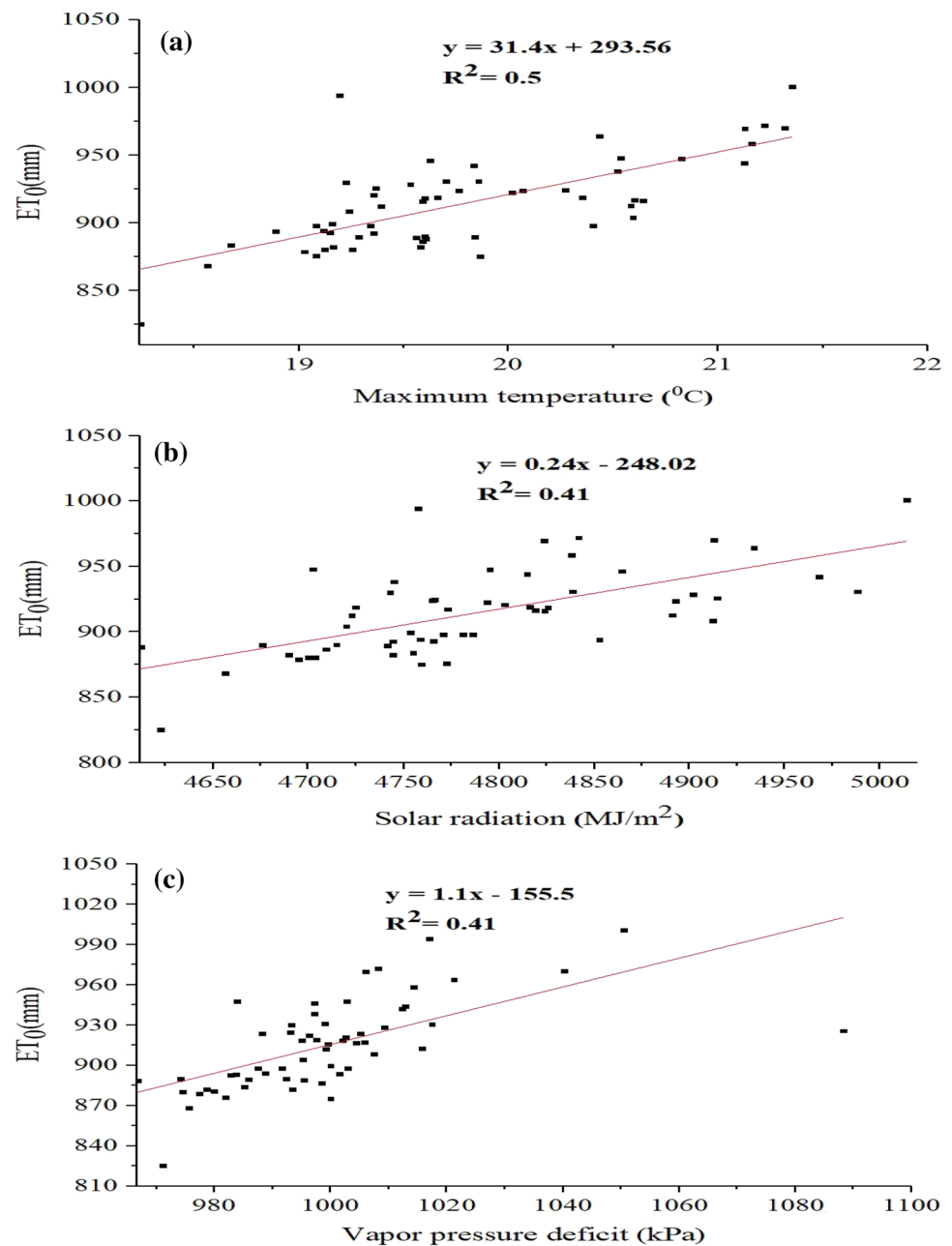
Fig. 5 (continued)



trend in 1984 and 2013. In 2013, the highest value of  $ET_0$  (1000 mm) was related to the highest value of the maximum temperature and solar radiation ( $21.35\text{ }^{\circ}\text{C}$  and  $5014\text{ MJ/m}^2$ ), respectively, however, which existed in the second highest value of the vapor pressure deficit ( $1050.4\text{ kPa}$ ). On the other hand, the lowest value of  $ET_0$  ( $840\text{ mm}$ ) was in 1968 which was similar to the lowest value of the maximum temperature ( $18.0\text{ }^{\circ}\text{C}$ ), the lowest value of solar radiation and vapor pressure deficit was in 1991. Annually scale, slope between  $ET_0$  and climate variables (maximum temperature, solar radiation and vapor pressure deficit) was  $31.4$ ,  $0.24$  and  $1.1\text{ mm/year}$ , respectively (Fig. 6).  $ET_0$  increased with the increase of climate variables, especially maximum temperature. The annual spatial distribution of  $ET_0$  illustrated a strong regional variation due to changes of different climate variables.  $ET_0$  is comparatively higher in the southwest of Yunnan Province, and decreases toward the Guizhou Province similar to the spatial distribution of maximum temperature, solar radiation, and vapor pressure deficit. While changes of wind speed were not significant, in general, the variations of annual and seasonal reference evapotranspiration of the study area reflect the comprehensive function of each climate parameters. Relative humidity or mean wind speed has a close relationship with reference evapotranspiration in most of the study area. The other parameters would enhance the impact of the major parameters according to their change and relation to reference evapotranspiration.

From the above-mentioned descriptions, climate variables differently influenced  $ET_0$  in terms of different timescales. In this section, we further illustrate correlations between  $ET_0$  and climate variables. Table 2 presents the correlation coefficients among annual and seasonal scale of  $ET_0$  and climatic parameters. Solar radiation, vapor pressure deficit, temperature, and wind speed have a positive correlation with  $ET_0$ . While the relative humidity has negative correlation with  $ET_0$ ,  $ET_0$  variations over most of southwest China are almost related to maximum temperature and solar radiation variations. Variations of  $ET_0$  over most regions are almost consistent with the variations of maximum temperature and solar radiation. It was observed that the correlation coefficients are  $0.58$  between annual  $ET_0$  and maximum temperature, and  $0.50$  between annual  $ET_0$  and solar radiation. Solar radiation contributes to seasonal  $ET_0$  variation with correlation coefficient in spring ( $0.55$ ) higher than in winter ( $0.24$ ). It further observed that  $ET_0$  was mostly influenced by solar radiation in winter and relative humidity in spring. From the analysis of Pearson correlation coefficient in Table 2, it is indicated that all climate variables contribute differently to  $ET_0$ , and maximum temperature was the most influential factor to  $ET_0$ , followed by solar radiation and vapor pressure deficit although the solar radiation is regarded as the most important driver for  $ET_0$  in most of regions in china. Our results revealed that changes of increasing rate in maximum temperature and vapor pressure deficit were higher than

**Fig. 6** Coupling analysis between annual evapotranspiration ( $ET_0$ ) and key climate variables over the past 60 years (1960–2016) (**a** relationship between evapotranspiration with maximum temperature, **b** relationship between evapotranspiration with solar radiation and **c** relationship between evapotranspiration with vapor pressure deficit)



those of wind speed and solar radiation, which resulted in an increased change of  $ET_0$ . Maximum temperature is the most important factor controlling the trend, markedly increased during the period of 1960–2016 resulting in increasing  $ET_0$ . Ultimately, the meteorological parameters impact on spatial distribution of  $ET_0$  (Yin et al. 2010a, b; Li et al. 2012).

### Spatiotemporal changes of ecosystem dynamics

To investigate the dynamics of ecosystem changes, we further established relationships between ecosystem classifications and NDVI values. NDVI has been commonly used to illustrate the ecosystem condition (Li et al. 2004; Mkhabela et al. 2011). Our finding of NDVI values for forest,

**Table 2** Pearson correlation coefficients between  $ET_0$  and meteorological factors

	Spring	Summer	Autumn	Winter	Year
$T_{ave}$	-0.345 <sup>NS</sup>	0.100 <sup>NS</sup>	0.163 <sup>NS</sup>	-0.017 <sup>NS</sup>	-0.061 <sup>NS</sup>
$T_{max}$	0.512 <sup>S</sup>	0.135 <sup>NS</sup>	0.439 <sup>S</sup>	0.278 <sup>NS</sup>	0.580 <sup>S</sup>
$T_{min}$	-0.761 <sup>S</sup>	-0.019 <sup>NS</sup>	-0.077 <sup>NS</sup>	-0.194 <sup>NS</sup>	-0.478 <sup>S</sup>
RH	0.699 <sup>S</sup>	0.070 <sup>NS</sup>	0.043 <sup>NS</sup>	0.196 <sup>NS</sup>	0.404 <sup>S</sup>
$R_s$	0.551 <sup>S</sup>	0.183 <sup>NS</sup>	0.277 <sup>NS</sup>	0.239 <sup>NS</sup>	0.501 <sup>S</sup>
VPD	0.423 <sup>S</sup>	0.175 <sup>NS</sup>	-0.198 <sup>NS</sup>	-0.216 <sup>NS</sup>	0.170 <sup>NS</sup>
WS	-0.345 <sup>NS</sup>	0.100 <sup>NS</sup>	0.163 <sup>NS</sup>	-0.017 <sup>NS</sup>	-0.061 <sup>NS</sup>

$T_{ave}$  is average temperature,  $T_{max}$  is maximum temperature,  $T_{min}$  is minimum temperature,  $RH$  is relative humidity,  $R_s$  is solar radiation,  $VPD$  is vapor pressure deficit and  $WS$  is wind speed

$P < 0.05$  ( $\alpha = 0.05$ ),  $S$  correlation is significant and  $NS$  correlation is not significant

agriculture, and grass ecosystem ranged from 0.55 to 0.56, 0.50 to 0.51, and 0.45 to 0.46, respectively (Fig. 7). More than 76% of the total area had NDVI values over 0.5 which was covered by forest and agriculture ecosystem Fig. 8. The highest and lowest NDVI values were in 2003 and 2000, i.e., 0.56 and 0.41, respectively. The highest NDVI in 2003 was consistent with the optimal climate in 2003 (Fig. 9). Forests in southwest of Yunnan Province, the east part of Guizhou Province and Sichuan Province was of the highest NDVI in these areas which reached to 0.63 in 2015 as average, and grass ecosystem had lower NDVI value than those ecosystems of agriculture and forests ecosystem (Fig. 7b). Seasonally, NDVI had a significant difference between wet and dry season. In the wet season, the lower value of NDVI (with less than 0.5) was covered by only 18% of the total study area that located in northwest of Sichuan and Yunnan Province, in contrast, the higher value of NDVI over than 0.5 was covered by around 82% of the total study area, e.g. eastern part of the study area (Fig. 7d). However, in the dry season, the lower value of NDVI (less than 0.5) was dominated in around 45% of the total area which concentrated especially in the northwest of Sichuan Province and small parts of Guizhou and Yunnan Province.

Spatial distribution of ecosystem types has a clear regional variety in southwest China, which was deeply influenced by climate, geomorphology, and hydrothermal distribution. The dominant ecosystem in southwest China

was forest (49%), grass (28%), and agriculture (23%) during 1980–2015 (Table 3). Fig. 8 shows the spatial distribution of ecosystem types from 1980 to 2015. Forest and grass were distributed primarily in the southern and eastern mountain areas, especially, the grass ecosystem was in high mountainous area (e.g., Sichuan plateau) while agriculture land was prevalent in basin areas. Transition matrix for the ecosystem type during 1980–2000 is illustrated in Table 4. The areas of agriculture and forest decreased by 999 km<sup>2</sup> and 2423 km<sup>2</sup>, respectively. Grass ecosystem increased 3740 km<sup>2</sup>. The area of forest converted to grass was 3670 km<sup>2</sup>, which was greater than transition from grass to forest (1720 km<sup>2</sup>). There was 819 km<sup>2</sup> agriculture area that converted into grass, and it was slightly greater than the grass area which was converted to agriculture (647 km<sup>2</sup>). The transition between grass ecosystem and other ecosystem was obviously higher than others, especially, in comparison with forest. Transition matrix of ecosystem types during 2000–2015 is illustrated in Table 5. Agriculture and grass were decreased by 4041 km<sup>2</sup> and 1716 km<sup>2</sup>, respectively. Forest increased slightly about 925 km<sup>2</sup> during 2000–2015. The area converted from grass to forest was 2237 km<sup>2</sup>, and it was greater than those area which was converted to grass (1299 km<sup>2</sup>). The converted areas from agriculture to forest (1109 km<sup>2</sup>) were greater than those from forest to agriculture (202 km<sup>2</sup>). Both cultivation of forest from grass and agriculture, and the transition areas between forest and other types were higher than others, especially, in comparison with agriculture ecosystem.

Changes of climate variables, especially temperature, precipitation, and moisture regimes, influenced much more on the distribution, growth, reproduction of ecosystem and variations in the types of ecosystem in the southwest of China. Climate variables changes impacted on grass and forest ecosystem resulted in the grass and forest ecosystem distributed in the southern and eastern mountain areas, and most grass ecosystem were existed in high mountains area (e.g., Sichuan plateau) while agriculture land located within the basin areas (e.g., Sichuan Basin and some parts in Guizhou province). Most recent studies indicated that climate is the major reason for the distribution of tropical forest and savanna at large spatial scales. Undoubtedly, the savanna was observed to be converted into forest when annual rainfall increased by 1500 mm and duration of seasonal drought was minimal. In our study, the uptrend temperatures and downtrend

**Fig. 7** Spatiotemporal change of NDVI and its relationship with ecosystems. **a** Temporal changes of annual NDVI from 2000 to 2015, **b** the NDVI of the ecosystem types, **c** spatial distribution of annual NDVI, **d** wet season and **e** dry season (The NDVI were classified as 8 levels, the lowest one was below 0.2 which means the lowest ecosystem condition and > 0.8 (from 0.8 to 1) means the highest ecosystem condition)

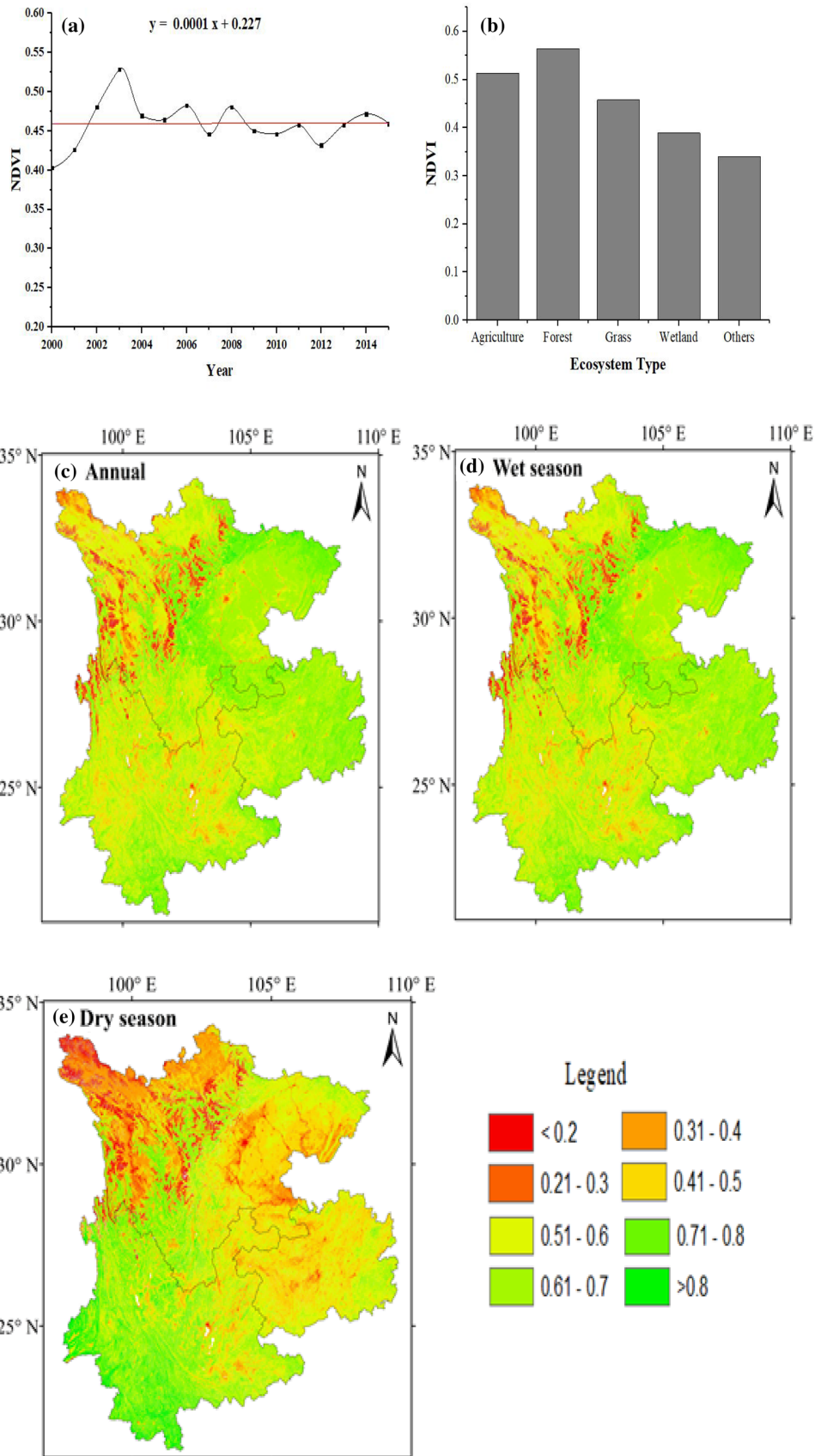


**Table 3** The ecosystem changes in southwest China during the period 1980–2015 (unit: km<sup>2</sup>)

	Agriculture	Forest	Grass	Wetland	Others
1980	240,471	479,351	289,681	13,163	19,365
1990	240,836	480,486	289,704	10,461	21,075
1995	234,031	486,652	289,802	10,198	21,732
2000	239,472	476,927	293,421	10,659	21,550
2005	238,293	478,179	292,570	10,721	7885
2010	237,471	478,691	292,299	10,867	22,704
2015	235,431	477,852	291,707	11,703	10,885
Percentage	22.93	46.22	28.06	1.07	1.72

precipitation especially the relatively large rising temperature played an important role in the decreasing of agriculture area from 2000 to 2015. Agriculture and grass were decreased although the forest was increased due to the impacts of climate changes during this period. There were many factors that were responsible to grass degradation, including consuming biomass energy, overgrazing and damage due to grass insects. The major driving forces in agriculture land decrease included water resource protection, urban expansion and implementation of ecological projects. In our research, the increased forest by 925 km<sup>2</sup> and decreased agriculture ecosystem by 4041 km<sup>2</sup> after 2000s were benefited from implementation of “Grain for Green Project” in southwest China.

Because of the environmental impacts during the past three decades from 1982 to 2012 in southwest China, the agricultural land decreases although evergreen forest and mixed forest had an increasing trend, especially in south of Yunnan province. Savannas increased from 1982 to 2002, then decreased after 2002 (Liu et al. 2014; He et al. 2017). On the other hand, there was a large area converted from agriculture to forest and grass ecosystem. However, from the year 2000 to 2010, forest ecosystem area increased by  $27.47 \times 10^4$  ha as a result of the  $34.19 \times 10^4$  ha of grass area converted to forest, another reason is the role of reforestation projects “Grain for Green” to increase the forested area by  $15.31 \times 10^4$  ha, so grass ecosystem area decreased by  $29.35 \times 10^4$  ha. Agriculture decreased by  $17.84 \times 10^4$  ha from 2000 to 2010 due to ecological restoration programs and urban construction in the agricultural area (Liu et al. 2014, Mokhtar et al. 2019). (Peng et al. 2011) indicated that

the agricultural area was increased from 41 to 46% during the period of 1973–1970 and then decreased to 38% in 2002 and changed a little in in Guizhou province from 1970 to 2007. Increase of population resulted to increase the area of agriculture of 8% during the period from 1990 to 2000; furthermore, forest and grass had a sharply decreasing trend in the same period.

### Coupling climate variability and ecosystem dynamics (2000–2015)

Ecosystem in southwest China was sensitive to the main meteorological parameters such as precipitation, temperature, and evapotranspiration. Ecosystem changes are the combination result of climate changes. Average NDVI was slightly increased by 0.0001 per year based on combined effects of climate variables and evapotranspiration. Temporal changes between annual NDVI and climate variables are shown in Fig. 9. The slope of the relationship between the NDVI with precipitation, temperature, and evapotranspiration was  $-1.01/\text{mm}$ ,  $0.01/^\circ\text{C}$ , and  $1.11/\text{mm}$ , respectively. The negative correlation between the NDVI and precipitation suggested that high precipitation reduced incoming solar radiation, and cloudy cover had negative effects on NDVI. However, seasonally, the temperature is a major factor controlling on NDVI variations more than precipitation did.

Spatial correlation was further analyzed between climate parameters and NDVI (Fig. 10). Precipitation and NDVI had a significantly negative correlation in the north of Sichuan, northwest of Yunnan provinces and center of Guizhou province (where karst landform dominates). Precipitation plays a vital role in NDVI through decreasing the incoming solar radiation which had negative effect on NDVI due to increased precipitation and cloudy cover in Yunnan and Sichuan provinces (Fig. 10a). There were positive correlations between climate variables and NDVI in southeast of Sichuan, eastern Yunnan and Guizhou Province. For example, the strong negative correlations among temperature and NDVI in the northwest Sichuan and west Yunnan Provinces were characterized by lower temperature and precipitation, especially in northwest Sichuan which covered by grass (Fig. 10b). Due to the cold temperature and deficit in precipitation, it led to grass degradation and low NDVI values. Most grass ecosystems, which were very sensitive to high temperature, were located in the northeast and southeast of Sichuan and some parts in Yunnan and Guizhou Provinces.

**Fig. 8** Spatial distribution analysis of ecosystem changes derived from NDVI in southwest China (1980–2015) (**a** 1980, **b** 1990, **c** 1995, **d** 2000, **e** 2005, **f** 2010, **g** 2015)

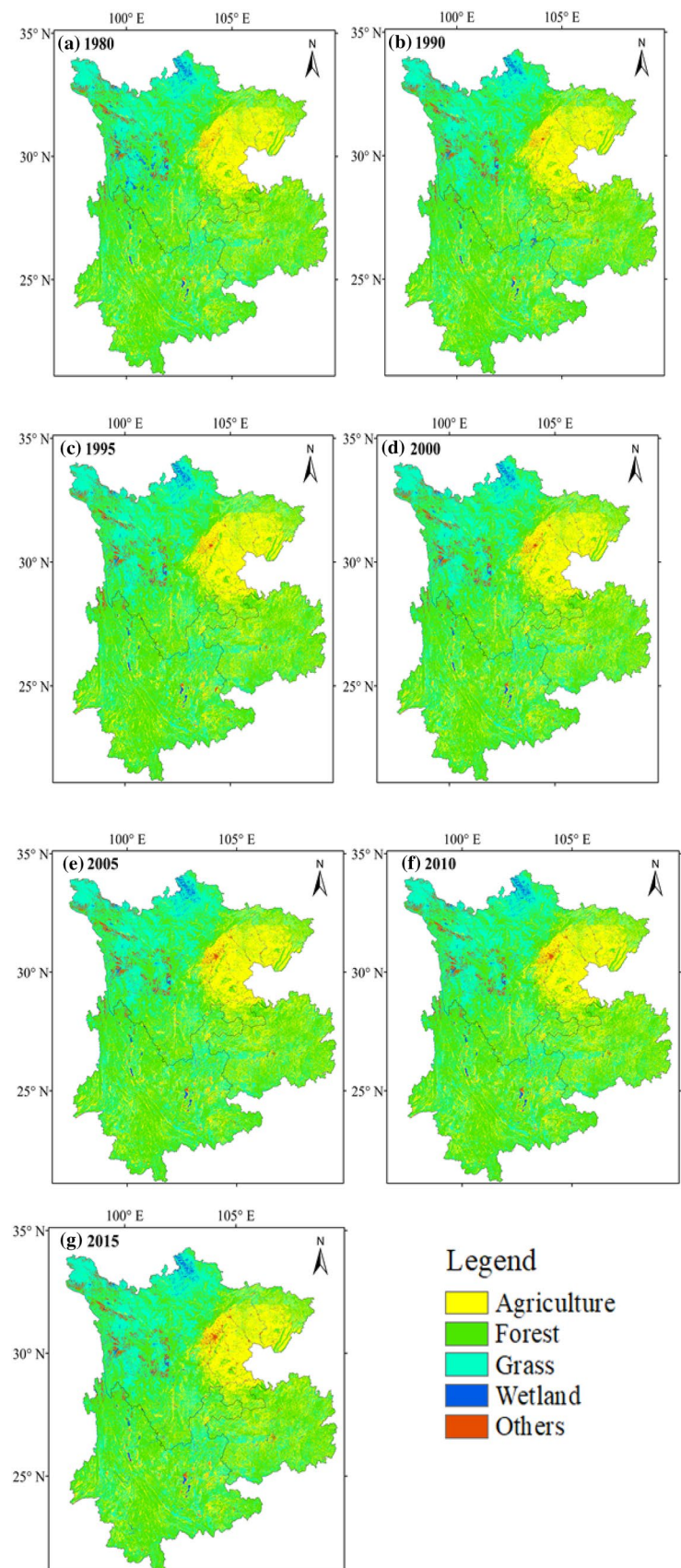




**Table 4** Transformation matrix for the ecosystem type in southwest China during 1980–2000 (unit: km<sup>2</sup>)

1980	2000					
	Agriculture	Forest	Grass	Wetland	Others	Total 1980
Agriculture	237,402	870	819	296	1084	240,471
Forest	1337	474,239	3670	46	58	479,350
Grass	647	1720	287,077	98	139	289,681
Wetland	70	93	1844	10,217	938	13,162
Others	16	1	5	2	19,331	4367
Total 2000	239,472	476,927	293,421	10,659	21,550	

Rows stand for ecosystem types in 1980, whereas columns mean that in 2000, each value in the transition matrix mean an ecosystem in 1980 (columns) transformed into another ecosystem in 2000 (rows)

**Table 5** Transformation matrix for the ecosystem type in southwest China during 2000 and 2015 (unit: km<sup>2</sup>)

2000	2015					
	Agriculture	Forest	Grass	Wetland	Others	Total 2000
Agriculture	234,747	1109	606	378	2632	239,472
Forest	202	474,488	1299	308	630	476,927
Grass	458	2237	289,728	435	563	293,421
Wetland	19	5	53	10,555	27	10,659
Others	4	4	5	10	21,487	21,550
Total 2015	235,431	477,852	291,705	11,702	25,339	

Rows stand for ecosystem types in 2000, whereas columns mean that in 2015, each value in the transition matrix means an ecosystem type in 2000 (columns) transformed into another ecosystem type in 2015 (rows)

However, the increasing temperature led to rise in evapotranspiration, and finally decline NDVI. The correlation coefficients between temperature and NDVI were positive in northeast of Sichuan province, southwest Yunnan and small parts in Guizhou province. Correlation coefficients between annual variations in evapotranspiration had significantly negative correlation with NDVI in most of Guizhou Province, particularly in the northern and southeastern parts of Sichuan Province. The agriculture was very sensitive to high temperature, and it was responsible to increase the potential evapotranspiration rate.

Ecosystem links the atmosphere, soil, and water resources, and it was an indicator of climate changes (Bonan and Pollard 1992; Cramer et al. 2001; Piao et al. 2005). The ecosystem sensitivity was related to climate variables, especially precipitation (Xu et al. 2008). The significant changes in precipitation and temperature during this period have affected the ecosystem in southwest China. Precipitation is the major factor controls in the productivity of the grass, increased precipitation leads to increase of grass productivity and vice versa. Furthermore, grass is more sensitive

to temperature, especially in the high-temperature areas (Li et al. 2008).

## Conclusion

Climate change is critical for the safety of water resources and ecological ecosystem changes. Our study aims to quantify the relationship between ecosystem and climate variables in southwest China through investigate  $ET_0$  variabilities and climatic variables ( $P$ ,  $T_{ave}$ ,  $T_{max}$ ,  $T_{min}$ , RH, WS,  $R_s$ , and VPD), and quantified relationships between ecosystem and climate variables. Therefore, the main conclusions were drawn as follows:

$ET_0$  has a significant change in the temporal and spatial distribution due to the complex in the topography condition and climate variables which contribute differently to  $ET_0$ , for example, maximum temperature was most contributor of  $ET_0$ , followed by solar radiation and vapor pressure deficit, respectively, however, low relative humidity contributed much more in enhancing  $ET_0$ , while low wind speed and

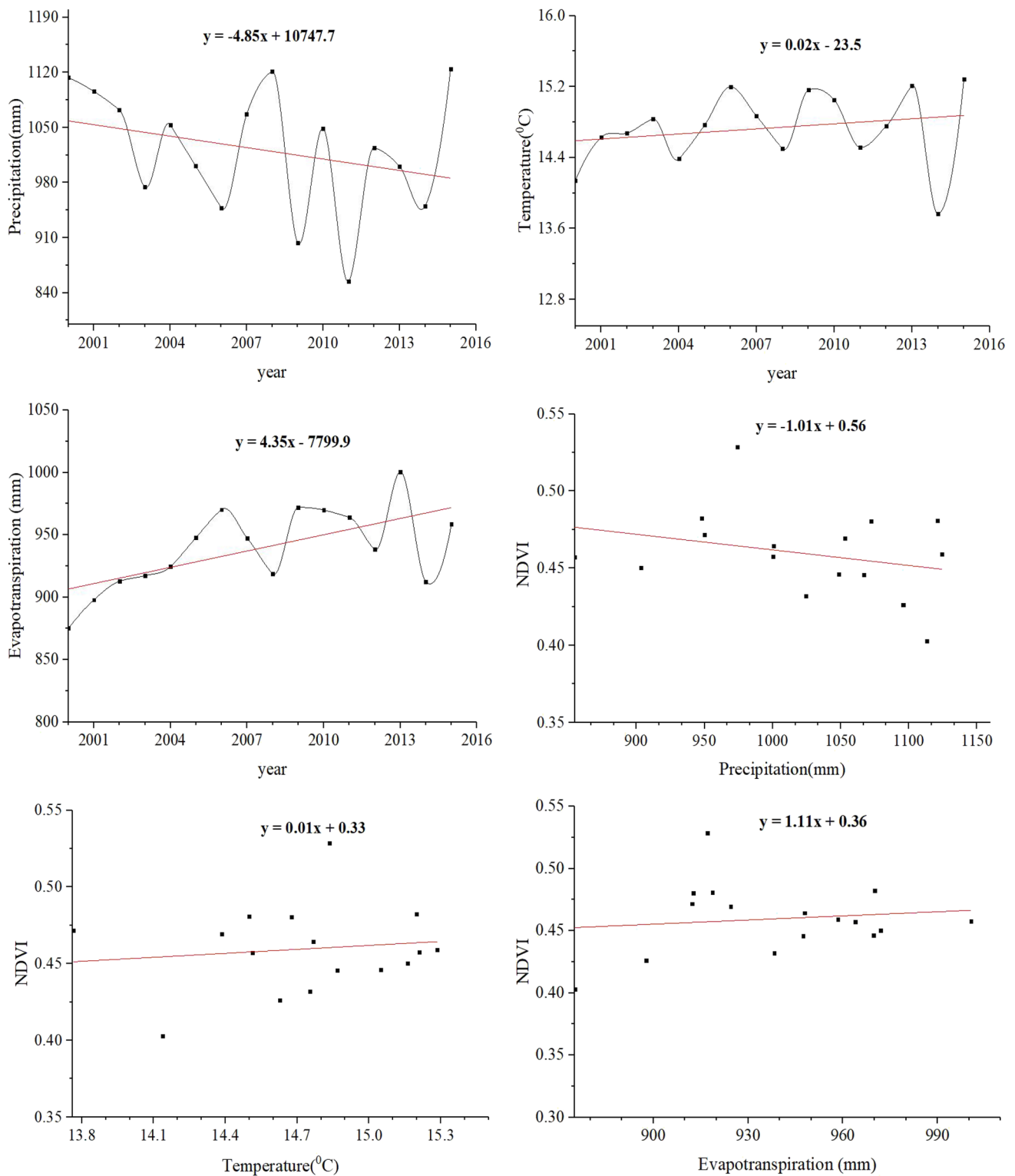


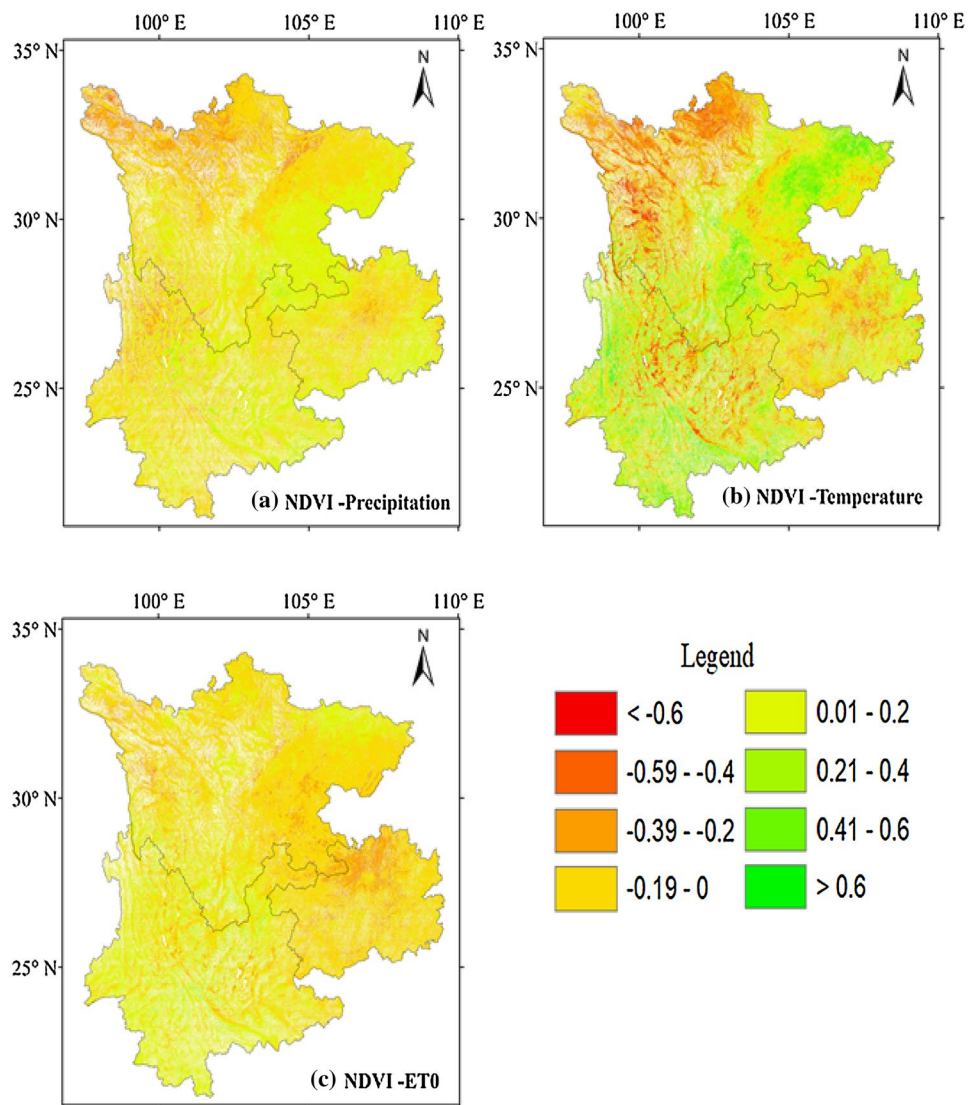
**Fig. 9** Time series analysis between climate variables and NDVI (2000–2015)

sunshine duration were responsible for the decrease of  $ET_0$ . Thus, southwest of Yunnan province was the highest increasing trend of  $ET_0$  based on the significantly increased of temperature and the decreasing trend of precipitation, sunshine

duration, wind speed, and relative humidity had from 1960 to 2016.

Climate and ecosystem feedbacks influenced greatly on distribution patterns of ecosystem, especially those of

**Fig. 10** Spatial distribution analysis between climate variables and NDVI (2000–2015) (a The spatial correlation between NDVI and precipitation, b the spatial correlation between NDVI and temperature and c the spatial correlation between NDVI and evapotranspiration)



forest, agriculture and grass ecosystem which were quite sensitive to the main meteorological parameters such as precipitation, temperature and evapotranspiration. Consequently, the highest and lowest NDVI values were in 2003 and 2000, respectively. Furthermore, human disturbances to natural forests and afforestation with several fast-growing tree species are harmful to native biodiversity and increase the system’s vulnerability to climate change. Moreover, the developing infrastructure to mitigate the impacts of water resources shortages, such as irrigation systems and reservoirs, we strongly suggest developing water-conserving agricultural techniques as adaptive strategies to climate change. Therefore, our further researches will focus much more on ecosystem biodiversity and river basin management, which will provide scientific evidence on hydrological processes and drought mitigation in southwest China as well as role of ecosystem biodiversity on water use efficiency.

**Acknowledgements** In this research, we are grateful for the assistance of anonymous reviewers and the editor for their invaluable comments to improve this paper. This article was financially supported by Projects of the National Key Research and Development Program (Grant No. 2017YFC0505200; 2017YFC0505205), the National Natural Science Foundation of China (Grant No. 41672180), the Project of the Integrated Scientific Expedition of the Ailao-Wuliang Mountains National Park (Grant No. 2019IB018), the Second Tibetan Plateau Scientific Expedition and Research Program (Grant No. SQ2019QZKK2003), the Strategic Priority Research Program of the Chinese Academy of Sciences (Grant No. XDA23020603), the Science & Technology Basic Resources Investigation Program of China (Grant No. 2017FY101303), the Key Platforms and Scientific Research Projects in Universities in Guangdong Province of China (Grant No. 2018KTSCX212) and the Guangdong Rural Science and Technology Commissioner Project of China (Grant No. 319B0203).

**Author contributions** AM collected the research data, analyzed data and writing—original draft preparation. AM and HH designed the research and provided suggestion to data analyses. AM and HZ generated the figures in the main text. AM, SK, CB, CZ, JW, QH, KA read and edited on the final manuscript. HH, YL, MA, KE contributed

greatly to the improvement of the final submission as well as the discussion of the revision work.

## References

- Allen MR, Ingram WJ (2002) Constraints on future changes in climate and the hydrologic cycle. *Nature* 419:224–232
- Allen RG (2000) Using the FAO-56 dual crop coefficient method over an irrigated region as part of an evapotranspiration inter comparison study. *J Hydrol* 229:27–41
- Allen RG, Pereira LS, Raes D, Smith M (1998) Crop evapotranspiration-Guidelines for computing crop water requirements-FAO irrigation and drainage paper 56. *Fao Rome* 300(9):D05109
- Bonan GB (2008) Forests and climate change: forcings, feedbacks, and the climate benefits of forests. *Science* 320(5882):1444–1449
- Bonan GB, Pollard D (1992) Vegetation on global climate. *Nature* 359:22
- Chen SB, Liu YF, Thomas A (2006) Climatic change on the Tibetan plateau: potential evapotranspiration trends from 1961 to 2000. *Clim Change* 76:291–319
- Chen XQ, Hu B, Yu R (2005) Spatial and temporal variation of phenological growing season and climate change impacts in temperate eastern China. *Glob Change Biol* 11:1118–1130
- Cramer W, Bondeau A, Woodward FI, Prentice IC, Betts RA, Brovkin V, Cox PM, Fisher V, Foley JA, Friend AD (2001) Global response of terrestrial ecosystem structure and function to CO<sub>2</sub> and climate change: results from six dynamic global vegetation models. *Glob Change Biol* 7(4):357–373
- DeWalle DR, Swistock BR, Johnson TE, McGuire KJ (2000) Potential effects of climate change and urbanization on mean annual stream flow in the United States. *Water Resour Res* 36:2655–2664
- Du J, Fang J, Xu W (2013) Analysis of dry/wet conditions using the standardized precipitation index and its potential usefulness for drought/flood monitoring in Hunan Province, China. *Stoch Env Res Risk Assess* 27:377–387
- Fabricante I, Oesterheld M, Paruelo JM (2009) Annual and seasonal variation of NDVI explained by current and previous precipitation across Northern Patagonia. *J Arid Environ* 73(8):745–753
- Fan ZX, Thomas A (2013) Spatiotemporal variability of reference evapotranspiration and its contributing climatic factors in Yunnan Province, SW China, 1961–2004. *Clim Change* 116:309–325
- Fang JY, Piao SL, He JS, Ma WH (2004) Increasing terrestrial vegetation activity in China, 1982–1999. *Sci China Life Sci* 47(3):229–240
- Feng L, Yang Q, Chen S, Luo Z, Fei Y, Wang R (2014) Temporal and spatial variability of sediment flux into the sea from the three largest rivers in China. *J Asian Earth Sci* 87:102–115
- Foley JA, DeFries R, Asner GP, Barford C, Bonan G, Carpenter SR, Chapin FS, Coe MT, Daily GC, Gibbs HK, Helkowski JH, Holloway T, Howard EA, Kucharik CJ, Monfreda C, Patz JA, Prentice IC, Ramankutty N, Snyder PK (2005) Global consequences of land use. *Science* 309:570–574. <https://doi.org/10.1126/science.1111772>
- Gao G, Chen D, Ren GY, Chen Y, Liao YM (2006) Spatial and temporal variations and controlling factors of potential evapotranspiration in China: 1956–2000. *J Geog Sci* 16(1):3–12
- Gao ZD, He JS, Dong KB, Bian XD, Li X (2017) Trends in reference evapotranspiration and their causative factors in the West Liao River basin, China. *Agric For Meteorol* 232:106–117
- Gemmer M, Becker S, Jiang T (2004) Observed monthly precipitation trends in China 1951–2002. *Theor Appl Climatol* 77:39–45
- Gobron N, Pinty B, Mélin F, Taberner M, Verstraete MM, Belward A, Lavergne T, Widlowski JL (2005) The state of vegetation in Europe following the 2003 drought. *Int J Remote Sens* 26:2013–2020
- Gong L, Xu CY, Chen D, Chen DL, Halldin S, Chen YD (2006) Sensitivity of the Penman-Monteith reference evapotranspiration to key climatic variables in the Changjiang (Yangtze River) basin. *J Hydrol* 329:620–629
- Goovaerts P (2000) Geostatistical approaches for incorporating elevation into the spatial interpolation of rainfall. *J Hydrology* 228:113–129
- Gu G, Adler RF, Huffman G, Curtis S (2007) Tropical rainfall variability on interannual-to interdecadal/longer-time scales derived from the GPCP monthly product. *J Clim* 20:4033–4046
- Han SJ, Xu D, Wang SL (2012) Decreasing potential evaporation trends in China from 1956 to 2005: accelerated in regions with significant agricultural influence? *Agric For Meteorol* 156:44A–56A
- Irmak S, Kabenge I, Skaggs KE, Mutiibwa D (2012) Trend and magnitude of changes in climate variables and reference evapotranspiration over 116-year period in the Platte River Basin, Central Nebraska–USA. *J Hydrol* 420–421:228–244
- Jackson RB, Carpenter SR, Dahm CN, McKnight DM, Naiman RJ, Postel SL, Running SW (2001) Water in a changing world. *Ecol Appl* 11:1027–1045
- Jhajharia D, Dinpashoh Y, Kahya E, Choudhary RR, Singh VP (2014) Trends in temperature over Godavari River basin in Southern Peninsular India. *Int J Climatol* 34:1369–1384
- Kendall MG (1955) Rank correlation methods. Hafner, New York
- Khanmohammadi N, Rezaie H, Montaseri M, Behmanesh J (2017) The effect of different meteorological parameters on the temporal variations of reference evapotranspiration. *Environ Earth Sci* 76:540
- Kjaersgaard JH, Plauborg F, Mollerup M, Petersen CT, Hansen S (2008) Crop coefficients for winter wheat in a sub-humid climate regime. *Agric Water Manag* 95:918–924
- Lehmann CER, Archibald SA, Hoffmann WA, Bond WJ (2011) Deciphering the distribution of the savanna biome. *New Phytol* 191:197–209
- Lewis SL (2006) Tropical forests and the changing earth system. *Philos Trans R Soc B* 361:195–210
- Li G, Zhou L, Wang D (2008) Variation of net primary productivity of grassland and its response to climate in Inner Mongolia (in Chinese with English abstract). *Ecol Environ* 17(5):1948–1955
- Li J, Heap AD (2008) Spatial interpolation methods: a review for environmental scientists. *Geoscience Australia, Canberra, Geoscience Australia, Record*
- Li J, Lewis J, Rowland J, Tappan G, Tieszen LL (2004) Evaluation of land performance in Senegal using multi-temporal NDVI and rainfall series. *J Arid Environ* 59(3):463–480
- Li XZ (2011) Long-term change in summer water vapor transport over South China in recent decades. *J Meteorol Soc Japan* 89A:271–282
- Li Z, Xu X, Yu B, Xu C, Liu M, Wang K (2016) Quantifying the impacts of climate and human activities on water and sediment discharge in a karst region of southwest China. *J Hydrol* 542:836–849
- Li Z, Zheng FL, Liu WZ (2012) Spatiotemporal characteristics of reference evapotranspiration during 1961–2009 and its projected changes during 2011–2099 on the Loess Plateau of China. *Agric For Meteorol* 154–155:147–155
- Li ZS, Liu GH, Fu BJ, Zhang JL (2011) The potential influence of seasonal climate variables on the net primary production of forests in Eastern China. *Environ Manage* 48(6):1173–1181
- Lin XS, Yu Q (2008) Study on the spatial interpolation of agroclimatic resources in Chongqing. *J Anhui Agric* 36(30):13431–13463, 13470
- Liu B, Chen C, Lian Y, Chen J, Chen X (2015) Long-term change of wet and dry climatic conditions in the southwest karst area of China. *Glob Planet Change* 127:1–11

- Liu CM, Zhang D, Liu XM, Zhao CS (2012) Spatial and temporal change in the potential evapotranspiration sensitivity to meteorological factors in China (1960–2007). *J Geog Sci* 22(1):3–14
- Liu JH, Wu JJ, Wu ZT, Liu M (2013) Response of NDVI dynamics to precipitation in the Beijing–Tianjin sandstorm source region. *Int J Remote Sens* 34(15):5331–5350
- Liu Y, Stanturf J, Lu H (2008) Modeling the potential of the northern China forest shelterbelt in improving hydroclimate conditions. *J Am Water Resour Assoc* 44:1176–1192
- Liu JY, Kuang WH, Zhang ZX, Xu XL, Qin YW, Ning J, Zhou WC, Zhang SW, Li RD, Yan CZ (2014) Spatiotemporal characteristics, patterns, and causes of land-use changes in China since the late 1980s. *J Geogr Sci* 24:195–210. <https://doi.org/10.1007/s11442-014-1082-6>
- Lu GY, Wong DW (2008) An adaptive inverse-distance weighting spatial interpolation technique. *Comput Geosci* 34(9):1044–1055
- Ma ZG, Ren XB (2007) Drying trend over China from 1951 to 2006. *Adv Clim Change Res* 3(4):195–200
- Mokhtar A, He H, Zhao H, Keo S, Bai C, Zhang C, Ma Y, Ibrahim A, Li Y, Li F, He W, Abdo AI, Zhou J (2019) Water resources risks and management strategy in River Basins of Hengduan Mountains, Southwest China. *Environ Sci Water Res Technol* 6:656–678. <https://doi.org/10.1039/C9EW00883G>
- Mann HB (1945) Nonparametric tests against trend. *Econometrica* 13:245–259
- Mantua N, Tohver I, Hamlet A (2010) Climate change impacts on streamflow extremes and summertime stream temperature and their possible consequences for freshwater salmon habitat in Washington state. *Clim Change* 102(1–2):187–223. <https://doi.org/10.1007/s10584-010-9845-2>
- Miao C, Ni J, Borthwick AG (2010) Recent changes of water discharge and sediment load in the Yellow River basin. *China Prog Phys Geog* 34:541–561
- Mkhabela MS, Bullock P, Raj S, Wang S, Yang Y (2011) Crop yield forecasting on the Canadian Prairies using MODIS NDVI data. *Agric For Meteorol* 151(3):385–393
- Moeletsi ME, Shabalala ZP, De Nysschen G, Walker S (2016) Evaluation of an inverse distance weighting method for patching daily and dekadal rainfall over the Free State Province. *South Africa. Water SA* 42(3):466–474
- Peng J, Xu YQ, Cai YL, Xiao HL (2011) The role of policies in land use/cover change since the 1970s in ecologically fragile karst areas of Southwest China: A case study on the Maotiaohe watershed. *Environ Sci Policy* 14:408–418
- Piao S, Fang J, Liu H, Zhu B (2005) NDVI-indicated decline in desertification in China in the past two decades. *Geophys Res Lett* 32:L06402. <https://doi.org/10.1029/2004GL021764>
- Piao SL, Fang JY, Ji W, Guo QH, Ke JH, Tao S, Woods K (2004) Variation in a satellite-based vegetation index in relation to climate in China. *J Veg Sci* 15(2):219–226
- Ray DK, Gerber JS, MacDonald GK, West PC (2015) Climate variation explains a third of global crop yield variability. *Nat Commun* 6(1):1–9. <https://doi.org/10.1038/ncomms6989>
- Sui Y, Jiang DB, Tian ZP (2013) Latest update of the climatology and changes in the seasonal distribution of precipitation over China. *Theoret Appl Climatol* 113:599–610
- Suleiman AA, Tojo Soler CM, Hoogenboom G (2007) Evaluation of FAO-56 crop coefficient procedures for deficit irrigation management of cotton in a humid climate. *Agric Water Manag* 91:33–42
- Sumner DM, Jacobs JM (2005) Utility of Penman–Monteith, Priestley–Taylor, reference evapotranspiration, and pan evaporation methods to estimate pasture evapotranspiration. *J Hydrol* 308:81–104
- Sun G, Alstad K, Chen JQ, Chen SP, Ford CR, Lin GH, Liu CF, Lu N, McNulty SG, Miao HX, Noormets A, Vose JM, Wilske B, Zeppel M, Zhang Y, Zhang ZQ (2011) A general predictive model for estimating monthly ecosystem evapotranspiration. *Ecohydrology* 4:245–255
- Suyker AE, Verma SB (2009) Evapotranspiration of irrigated and rainfed maize–soybean cropping systems. *Agric For Meteorol* 149:443–452
- Thomas A (2008) Agricultural irrigation demand under present and future climate scenarios in China. *Global Planet Change* 60:306–326
- Tony P (2008) Conceptual framework for assessment and management of ecosystem impacts of climate change. *Ecol complex* 5:329–338
- Wang J, Meng JJ, Cai YL (2008) Assessing vegetation dynamics impacted by climate change in the southwestern karst region of China with AVHRR NDVI and AVHRR NPP time-series. *Environ Geol* 54(6):1185–1195
- Wang Y, Zhou G (2010) Evapotranspiration characteristics and crop coefficient of rain-fed maize agroecosystem. *Chin J Appl Ecol* 21:647–653 (in Chinese)
- Xu X, Chen H, Levy JK (2008) Spatiotemporal vegetation cover variations in the Qinghai–Tibet Plateau under global climate change. *Chin Sci Bull* 53(6):915–922
- Xu X, Du YG, Tang JP, Wang Y (2011) Variations of temperature and precipitation extremes in recent two decades over China. *Atmos Res* 101:143–154
- Ye JS, Li WB, Li LF, Zhang F (2013) “North drying and south wetting” summer precipitation trend over China and its potential linkage with aerosol loading. *Atmos Res* 125:12–19
- Yin YH, Wu SH, Chen G, Dai EF (1960s) Attribution analyses of potential evapotranspiration changes in China since the 1960s. *Theor Appl Climatol* 101:19–28
- Yin YH, Wu SH, Dai EF (2010b) Determining factors in potential evapotranspiration changes over China in the period 1971–2008. *Chin Sci Bull* 55(29):3329–3337
- Yu F, Cui N, Lu Z, Gong D, Zhang K (2017) Spatiotemporal variation of reference evapotranspiration during 1954–2013 in Southwest China. *Quatern Int* 441:S1040618216300635
- Zhai PM, Zhang XB, Wan H, Pan X (2004) Trends in total precipitation and frequency of daily precipitation extremes over China. *J clim* 18:1096–1108
- Zhang D, Liu XM, Hong HY (2013) Assessing the effect of climate change on reference evapotranspiration in China. *Stoch Env Res Risk Assess* 27:1871–1881
- Zhang FM, Shen SH (2007) Spatial distribution and temporal trend of reference crop evapotranspiration in China. *J Nanjing Inst Meteorol* 30(5):705–709
- Zhu HY, Jia SF (2004) Uncertainty in the spatial interpolation of rainfall data. *Prog Hum Geogr* 23(2):34–42